Available online at www.sciencedirect.com
ScienceDirect
Tribology International 40 (2007) 924–929
TRIBOLOGY INTERNATIONAL
www.elsevier.com/locate/triboint

Reduction of three-dimensional contact problems to one-dimensional ones

T. Geike*, V.L. Popov

Technische Universität Berlin, Str. des 17 Juni 135, 10623 Berlin, Germany

Available online 19 April 2006

Abstract

It is shown that three-dimensional contacts have the same force–displacement law as in a simple one-dimensional model. This is valid both for normal and tangential contact problem. Under some additional assumptions these ideas can be used for adhesive contacts too. The above reduction makes it possible to develop effective simulation methods for contact and friction processes.

Keywords: Contact mechanics model; Elastic contact; Adhesion; Simulation model

1. Introduction

Macroscopic tribological systems are typically multi-contact systems. The micro contact configuration determines on one hand the normal forces between bodies, which we macroscopically perceive as reaction forces. On the other hand, they determine the "real" contact area and thus the tangential friction forces. The distribution of normal and tangential forces as well as distribution of contact areas of micro contacts are the most important quantities for understanding and qualitative characterisation of tribological systems on the microscale. The multi-contact and multi-scale nature of friction processes makes it difficult to simulate such systems numerically. It is therefore important to develop reduced simulation methods. One of the possibilities to reduce the computation time is to use hierarchical simulation methods. In the present paper, another strategy is discussed: substitution of three-dimensional (3D) systems by systems with reduced dimension.

For the purpose of motivation the normal contact without adhesion is examined (Section 2). Then the model with adhesion will be described in some detail (Section 3). Results regarding the normal contact with adhesion and the parameter identification are presented in Section 4. Finally some preliminary comments on the tangential contact problem and friction are made.

2. Normal contact without adhesion

Let us consider the non-adhesive contact between two elastic spheres. Hertz theory [1] gives the elastic energy

$$U_{3D} = \frac{4\sqrt{2}G}{15(1-\nu)}\sqrt{Rd^5}, \tag{1}$$

where R is the radius of curvature, d the penetration, G the shear modulus and ν Poisson's ratio (Fig. 1a). We would like to find out if the 3D non-adhesive normal contact problem can be modelled on the basis of a one-dimensional (1D) model. The contact between an elastic layer that is attached to a rigid cylinder (Fig. 1b) and a rigid plane is described by the elastic energy

$$U_{1D} = \frac{2\sqrt{2}c_n}{15}\sqrt{Rd^5}, \tag{2}$$

where c_n is the (constant) stiffness of the layer per unit length. The two expressions are identical if the stiffness is chosen as

$$c_n = \frac{G}{2(1-\nu)}. \tag{3}$$

The elastic layer (continuum) can be further discretised by particles that are attached to the rigid cylinder by

*Corresponding author.

0301-679X/$ - see front matter © 2006 Elsevier Ltd. All rights reserved.
doi:10.1016/j.triboint.2006.02.035

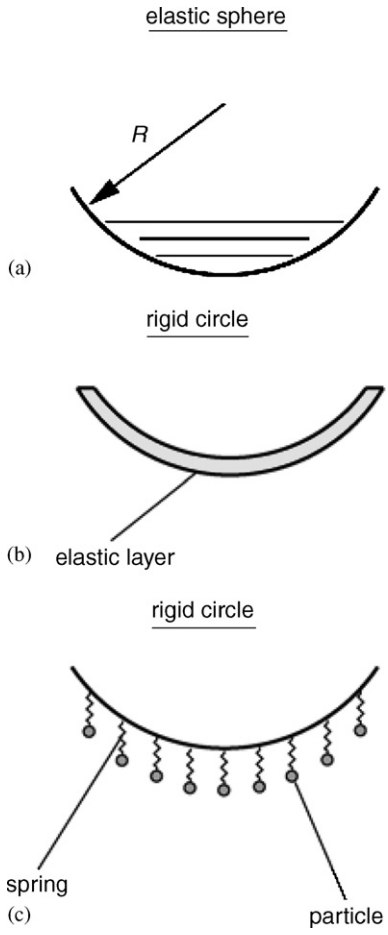

Fig. 1. Normal contact without adhesion: (a) elastic sphere (3D), (b) rigid cylinder/circle with elastic layer (1D), (c) particles attached to a rigid cylinder/circle by means of springs (1D).

springs. The stiffness of one of the springs (Fig. 1c) is the value c_n times the distance between any two springs. Thus we finally come to a 1D system with the same force–displacement dependence as for initial 3D system.

For the non-adhesive contact the parameter specifying the elastic interaction is independent of the radius of curvature and thus applicable to a surface with arbitrary form.

3. Normal contact with adhesion

3.1. Model description

Fig. 2 shows the model under consideration. Each particle has two degrees of freedom (horizontal and vertical). The same is true for the upper plate. The lower plate is fixed. Fig. 3 helps to understand the interactions between the particles and between the particles and the bulk. Each particle interacts with the bulk by means of a linear spring (Fig. 3a). Neighbouring particles are also connected by linear spring having transverse rigidity (Fig. 3b). Furthermore, each particle interacts with

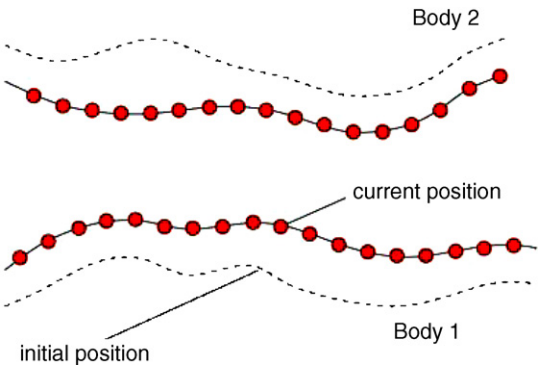

Fig. 2. Model under study: particles have two degrees of freedom, lower plate (body 1) is fixed.

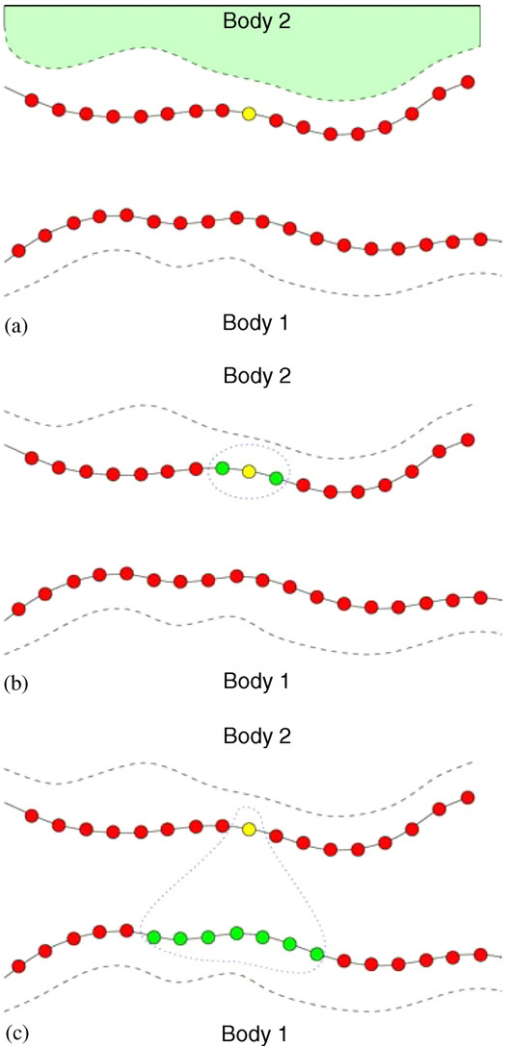

Fig. 3. Interactions: (a) between each particle and the bulk (linear springs), (b) between neighbouring particles (linear springs), (c) between particles from different bodies (non-linear interaction force).

particles of the opposite plate (Fig. 3c). In the simulation under study the potential is made up of two exponential functions (finite core). Two dynamic equations for each

particle (horizontal and vertical) can be written as

$$m_{i,k}\ddot{x}_{i,k} = F^x_{i,k}, \quad m_{i,k}\ddot{z}_{i,k} = F^z_{i,k}. \tag{4}$$

$m_{i,k}$ is the mass of the particle i on plate $k = 1, 2$. The forces on the right-hand side include the interactions between particles and between particles and bulk, viscose damping, stochastic forces (thermal fluctuations) and the interaction with an external driving cantilever (velocity, external force). Furthermore, two dynamic equations for the upper plate must be written ($k = 2$)

$$M_k\ddot{X}_k = F^X_k, \quad M_k\ddot{Z}_k = F^Z_k. \tag{5}$$

M_k is the total mass of the upper plate, X_k and Z_k are the position of the center of mass of the upper plate.

It is clear that the discrete 1D model will in general behave different than a 2D or a 3D continuum system. It is an important task to find the aspects of the "real world" that can be modelled with the proposed 1D model. As shown before the proposed model is suited to study the 3D non-adhesive normal contact problem, but it may not be suited for the adhesive contact. Further calculations will help to identify limitations of the reduced model. Moreover results for the normal contact problem will be the basis of the parameter identification. The macroscopic parameters encountered in the normal contact problem are the elastic modulus and the work of adhesion. The parameters may depend on the length scale or radius of curvature.

3.2. JKR theory

The solution for the adhesive contact between elastic spheres is given by Johnson et al. [2]. The adhesion force F_A is proportional to the radius of curvature R and does not depend on the elastic properties, i.e.

$$F_A = -3\pi\gamma R, \tag{6}$$

with the work of adhesion γ. The stress distribution is singular at the edge of the contact. In reality the singularity disappears due to the finite range of the interaction forces. The critical radius is

$$a_{cr} = \sqrt[3]{\frac{9\pi\gamma R^2}{4E^*}}, \tag{7}$$

where E^* is the effective elastic modulus. The relation between the applied force and the radius of contact can be written in non-dimensional variables as

$$\tilde{F} = 4\tilde{a}^3 - 4\tilde{a}^{3/2}, \tag{8}$$

with $\tilde{F} = F/F_A$ and $\tilde{a} = a/a_0$. The contact radius under the action of the external force $F = 0$ is called a_0.

The JKR theory applies to large, compliant spheres, while DMT theory is more appropriate for small, stiff spheres [3]. A parameter μ is introduced which can be understood as the ratio of elastic displacement of the surfaces at the point of separation to the effective range of surfaces forces. JKR theory is valid for large values of μ. Johnson and Greenwood [3] point out that JKR theory gives good results for the contact radius and contact stiffness even outside of the actual range of validity.

The radius of contact a has already been mentioned, but how to define the radius of contact in the particle model? Forces acting on each particle (caused by the opposite plate) give the pressure distribution. Since the range of interaction forces is finite no singularity appears. Greenwood [4] speaks of the contact radius as an ill-defined concept. He emphasises that once the tensile region is entered the only distinctive point is the maximum tensile stress. Thus we define the contact radius a as radius of maximum tensile stress (Fig. 4).

3.3. Numerical experiments

The setup (Fig. 5) is as follows: two surfaces, one is flat and fixed (body 1), the other one is curved and can move in vertical direction (body 2). In the first load step a compressive force F_D is applied to the upper plate. The upper plate will move downwards. Finally an equilibrium position is reached. Note that the equilibrium position is determined by a dynamic simulation.

Now a tensile force F_Z is applied and velocity and acceleration of the upper plate are observed. If a static equilibrium is reached the applied tensile force is smaller than the adhesion force. Iterating eventually yields the adhesion force and the critical radius.

Many numerical experiments have been performed. First the question whether the adhesion force and the critical radius depend on the compressive force F_D that had been applied initially is considered. In the JKR theory adhesion force F_A and critical contact radius a_{cr} do not depend on the applied compressive force F_D. In the numerical experiments a weak dependence of F_A and a_{cr} on F_D is observed (Fig. 6). F_A and a_{cr} are normalised by the respective mean values $\bar{F}_A$ and $\bar{a}_{cr}$.

JKR theory predicts a linear relation between adhesion force F_A and radius of curvature R (Eq. (6)). The model under study however yields $F_A \propto \sqrt{R}$ (Fig. 7a). Furthermore, the relation between the contact radius a_0 without external force and the radius of curvature R is established as $a_0 \propto \sqrt{R}$ (Fig. 7b), while JKR theory predicts $a_0 \propto R^{2/3}$ (Eq. (7)). Note that Barquins [5] results for the 2D continuum problem read $F_A \propto R^{1/3}$ and $a_0 \propto R^{2/3}$. The relations between F_A, a_0 and the radius of curvature R differ from JKR results (3D) and Barquins results (2D).

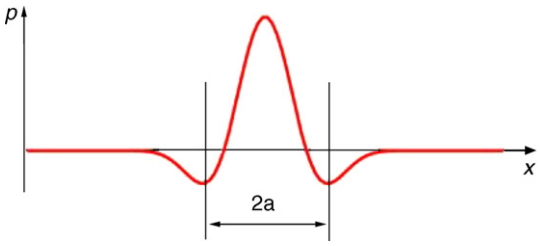

Fig. 4. Definition of contact radius.

Next the relation between external force F and radius of contact a is studied in more detail. The diagram (Fig. 8) shows the external force normalised by the adhesion force versus the contact radius normalised by the contact radius at 0 force. JKR theory gives a unique relation (8) that does not contain any parameters (e.g. radius of curvature, elastic modulus, work of adhesion).

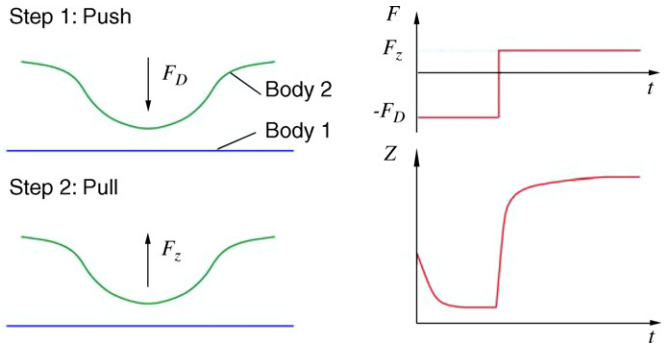

Fig. 5. Setup for numerical experiments, lower plate (body 1) is fixed.

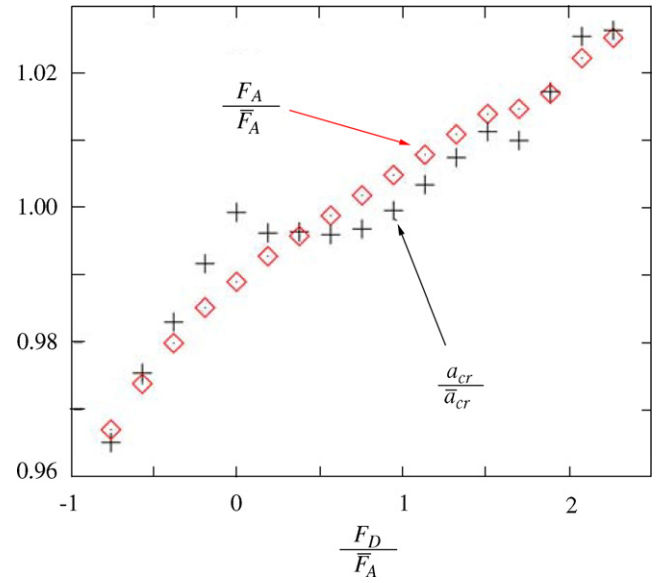

Fig. 6. Relation between force F_D initially applied and adhesion force F_A, critical radius a_{cr}.

Different numerical experiments with different numbers of particles yield curves close to the JKR curve (Fig. 8a). An increasing number of particles everything else being constant should not change the result whatsoever. More interesting is the variation of the radius of curvature. Once again curves close to the JKR curve are obtained (Fig. 8b).

It turns out that for arbitrary N and R fitting on the basis of 3D theory (JKR) suits results much better than fitting on the basis of the 2D theory (Barquins).

The results of the numerical experiments can be summarised as follows:

- The relations between F_A, a_0 and the radius of curvature R differ from JKR results (3D).
- $\tilde{F}$–$\tilde{a}$-curves lie on JKR-curve for every N and R (within a reasonable range of values).

Therefore the 3D static normal contact problem (with adhesion) can be simulated by the proposed 1D model for arbitrary but fixed R. Surfaces with fixed R and stochastic height distribution had been studied extensively by Greenwood and Williamson [6].

4. Parameter identification

The model contains many parameters, defining the interactions and inertia properties. Nothing has been said yet about how to relate them to the macroscopic material parameters. Since the relation between external force and radius of contact established in many numerical experiments equals the JKR result, parameter identification is based on the JKR theory, i.e.

$$\gamma = \frac{F_A}{3\pi R}, \quad E^* = \frac{3F_A R}{a_0^3}. \tag{9}$$

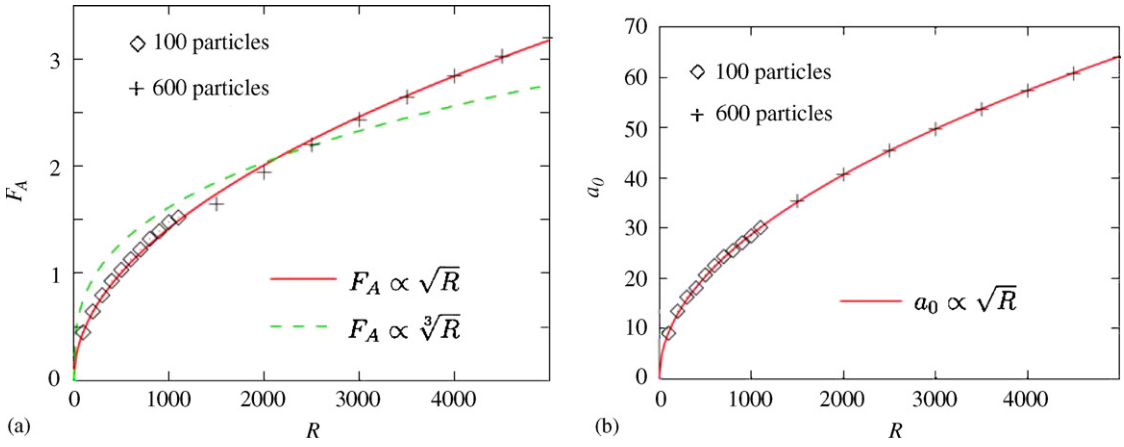

Fig. 7. Relation between radius of curvature R and (a) adhesion force F_A and (b) critical radius a_{cr}.

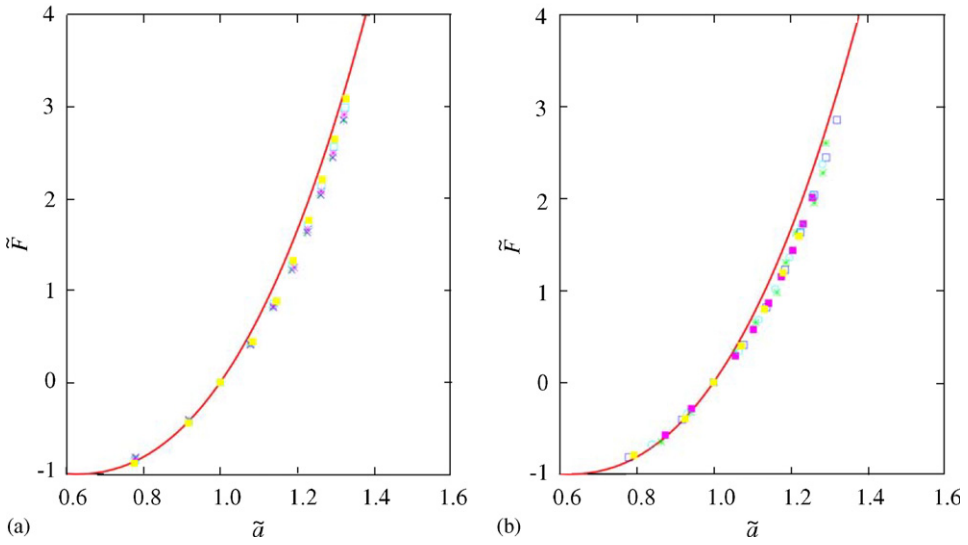

Fig. 8. Relation between applied force and contact radius: numerical experiments with (a) different numbers of particles, (b) different radii of curvature.

Table 1
Parameter identification: internal length and force scale are calculated for given macroscopic material parameters

N	R (LU)	a_0 (LU)	F_A (FU)	LU (nm)	FU (μN)
200	1000	28.53	1.47	6.1	39.0
200	1600	36.14	1.87	7.7	61.8
200	2000	40.36	2.09	8.6	77.6

Adhesion force and radius of contact without external force can be used to determine work of adhesion γ and elastic modulus E^*. Note that because $F_A \propto \sqrt{R}$ and $a_0 \propto \sqrt{R}$ work of adhesion does depend on R, but elastic modulus does not.

Table 1 gives an example. Radius of curvature and contact radius are measured in units of the equilibrium (trial position) distance between two particles, here called length unit (LU). The adhesion force is measured in some force unit (FU). Given some macroscopic values for the work of adhesion and the elastic modulus (here $E^* = 200\,\mathrm{GPa}$ and $\gamma = 1\,\mathrm{N\,m^{-1}}$) and one set of interaction parameters the length and force scale can be calculated for every radius of curvature.

Based on experimental results Popov and Starcevic [7] conclude that for the steel–steel pair under investigation the characteristic scale producing the maximum contribution to the microscopic interaction potential is about 50 nm. Thus values shown in Table 1 seem to be reasonable, since particle distance is about one order of magnitude smaller than the characteristic wavelength.

Furthermore, the mean pressure can be calculated, e.g. for $R = 1000$, $a = 35$ the mean pressure is about 800 MPa.

The elastic modulus does not depend on the radius of curvature. As long as the parameters which govern the interaction forces remain unchanged the same elastic modulus appears. For the adhesive contact the radius of curvature is very important, because the work of adhesion depends on it. Note that the number of particles has to be chosen appropriately. The contact region should be smaller than the chain.

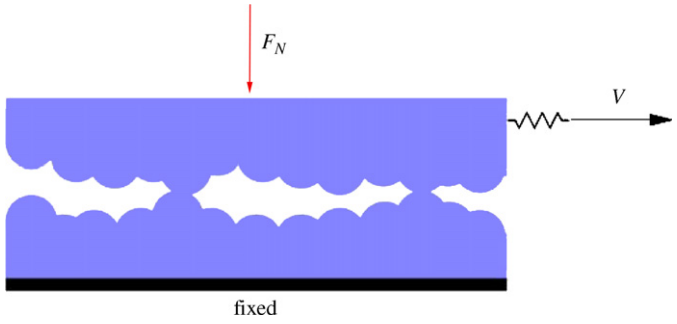

Fig. 9. Setup for the friction experiment.

5. Summary

The 3D static normal contact problem (with adhesion) can be simulated by the proposed 1D model for arbitrary but fixed radius of curvature. The authors believe that it can also be used for the study of friction problems.

The model is very simple and thus has a computational advantage over more sophisticated methods. The drawbacks arise from the simplicity. First of all only one length scale is considered, while often the fractal nature of surfaces is emphasised. However, experimental results (tribospectroscopy) suggest that for steel–steel-contact (and maybe other pairs as well) the major contribution to the friction force comes from one characteristic scale.

A second problem is interpenetration. Since only one layer is considered interpenetration arises at high compressive forces. In real solids, layers below the surface layer prevent the particles from the opposite body from penetrating.

Besides further improving the model and improving the understanding of how the parameters (e.g. interaction potential) influence the results, the study of the tangential contact problem and friction is the main topic. Later the model can be utilised to study the influence of material and loading parameters on friction force related to an actual technical problem (Fig. 9).

References

[1] Hertz H. Über die Berührung fester elastischer Körper. Z Angew Math 1882;92:156–71.

[2] Johnson KL, Kendall K, Roberts AD. Surface energy and contact of elastic solids. Proc R Soc London, Ser A 1971;324(1558):301.

[3] Johnson KL, Greenwood JA. An adhesion map for the contact of elastic spheres. J Colloid Interface Sci 1997;192:326–33.

[4] Greenwood JA. Adhesion of elastic spheres. Proc R Soc London, Ser A 1997;453(1961):1277–97.

[5] Barquins M. Adherence and rolling kinetics of a rigid cylinder in contact with a natural rubber surface. J Adhes 1988;26:1–12.

[6] Greenwood JA, Williamson JB. Contact of nominally flat surfaces. Proc R Soc London, Ser A 1966;295(1442):300.

[7] Popov VL, Starcevic J. Tribospectroscopic study of a steel–steel friction couple. Tech Phys Lett 2005;31(4):309–11.